Thermal evolution and electrical correlation of defect states in Hf-based high-κ dielectrics on *n*-type Ge (100): Local atomic bonding symmetry

K. B. Chung,[1,a)] J. P. Long,[2] H. Seo,[2] G. Lucovsky,[2,b)] and D. Nordlund[3]
[1]*Department of Physics, Dankook University, Dongnamgu Anseodong 29, Cheonan 330-714, Republic of Korea*
[2]*Department of Physics, North Carolina State University, Raleigh, North Carolina 27695-8202, USA*
[3]*Stanford Synchrotron Radiation Lightsource, Menlo Park, California 94025, USA*

(Received 9 June 2009; accepted 20 August 2009; published online 5 October 2009)

The crystal field splittings and Jahn–Teller (J-T) distortions in Hf-based high-κ dielectric oxides on *n*-type Ge (100) substrates were investigated through the examination of O K_1 edge spectra, obtained via x-ray absorption spectroscopy. Second derivative analysis of these O K_1 edge spectra provided unambiguous evidence of J-T *d*-state degeneracy removal, resulting from the symmetry of the local atomic bonding environment. Additionally, two distinct defect states were found below the conduction band edge. The conduction band's molecular orbital energy structure, including defect states, was determined based on the results of these investigations. Moreover, the thermal evolution of the defect states was found to be dependent on both postdeposition annealing temperature and Hf-based high-κ dielectric oxides. These subband-edge defect states were determined to be electrically active, and their density and the local atomic bonding symmetry were found to be correlated with the effective electron charge trapping measured in related device structures.
 [doi:10.1063/1.3236679]

I. INTRODUCTION

The aggressive scaling of Si-based complementary metal-oxide semiconductors has introduced a need to overcome several physical limitations to device performance. As a result, various attempts have been introduced to improve device properties by enhancing carrier mobility in the channel region and by modifying the channel structure[1–3] One promising solution to such difficulties involves modifying the Si channel region presently employed by an alternative semiconductor substrate or channel material, such as Ge, SiGe, or GaAs.[1–3] Ge, for example, has attracted considerable interest in this regard because of its significantly higher intrinsic carrier mobility and smaller band gap relative to Si. These properties provide a number of advantages to device performance, leading to improvements in injection current density, supply voltage scaling, faster switching speeds, and lower power consumption.[4] Despite having such desirable intrinsic properties, the fabrication of Ge-based devices has faced many difficulties, including the absence of a stable interface passivation oxide, an inherently low thermal budget, and a high defect density.[5]

Several research groups have attempted to apply high-κ gate oxides to Ge substrates and have used various interfacial treatments in efforts to obtain a stable oxide layer.[1,3,6] These studies, however, have reported that such devices still demonstrate relatively high defect densities, on the order of $\sim 10^{12}$ cm^{-2} following their fabrication.[3] These defect states in high-κ oxides and their interface function as electrical traps, which can induce electron and/or hole trapping.[7] In addition, higher electrical trap densities potentially present significant limitations to the operation and reliability of such devices.[8] Therefore, identifying the origins of defect states and measuring their correlation to electrical properties are crucial to the resolution of several delicate problems regarding Ge-based devices.

In this letter, we present the effects of crystal field (C-F) splittings and Jahn–Teller (J-T) distortions on the conduction bands of HfO_2 and HfSiON high-κ dielectric oxides deposited on *n*-type Ge (100) substrates. A thorough study, which includes the energy assignments of molecular orbital features, has been performed through second derivative analysis of O K_1 edge spectra, obtained through x-ray absorption spectroscopy (XAS). In addition to the interpretation of C-F splitting and J-T *d*-state degeneracy removal, we focus on the defect states below the conduction band edge. The evolution of defect states shows a dependence on both the given thermal energy and the structural stability of the material. These spectroscopically observed defect states are identified as electrically active and are correlated with the effective electron charge trapping.

II. EXPERIMENT

In efforts to minimize native oxide formation and to produce a flat Ge surface, an *n*-type Ge (100) wafer was rinsed sequentially with de-ionized water, H_2O_2 (6%), methanol, NH_4OH (15%), and de-ionized water.[9] Right after this surface treatment, a sacrificial, plasma-nitrided interfacial layer (GeN_x) was deposited by a remote plasma-enhanced metal-organic chemical vapor deposition (RPE-MOCVD) at 300 °C, followed immediately by the analogous deposition of a high-κ oxide film. The sacrificial GeN_x layer had a

a)Authors to whom correspondence should be addressed. Electronic mail: kbchung@dankook.ac.kr.
b)Authors to whom correspondence should be addressed. Electronic mail: lucovsky@ncsu.edu.

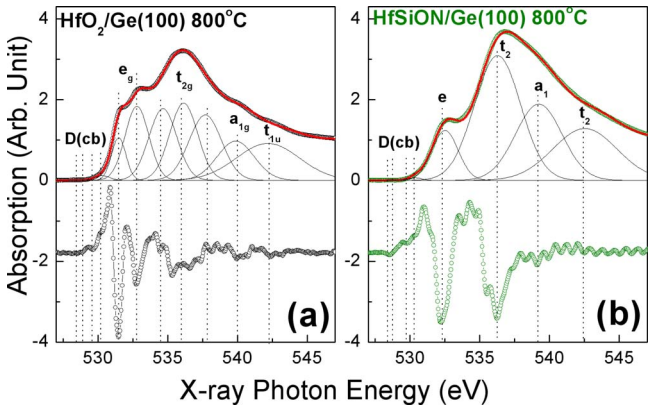

FIG. 1. (Color online) Normalized XAS O K_1 edge spectra in the upper figure (a) HfO_2 on Ge and (b) HfSiON on Ge annealed at 800 °C. Second derivative O K_1 edge spectra are in the bottom of figure, respectively. The Gaussian fits, which the energy positions were determined by the minimum of second derivative, represent the C-F splittings and the J-T *d*-state degeneracy removal. The molecular orbital indexes of each Gaussian fit are assigned by the symmetry of bonding environment based on the group theory. The defect states below the conduction band edge around 530 eV are detected from second derivative spectra and their Gaussian fits are considered as well.

thickness of 0.7 ± 0.1 nm and was deposited in order to prevent direct reaction between the Ge substrate and the high-κ overlayer, as well as to prevent substrate oxidation during the high-κ film deposition process. Following deposition, the samples were moved *in situ* into an online Auger electron spectroscopy chamber, in which the film composition was measured. *Ex situ* postdeposition annealing (PDA) was then carried out via one-minute rapid thermal anneals in an inert Ar ambient with temperatures ranging from 550 to 800 °C. Following sample fabrication, x-ray photoemission spectroscopy, spectroscopic ellipsometry, and medium energy ion scattering characterizations were conducted in order to investigate several physical characteristics of the oxide films. In order to observe detailed conduction band features, XAS measurements were also performed using the coherent x-ray beam at the Stanford Synchrotron Radiation Lightsource BL 10–1. Electrical properties were determined by measuring metal oxide semiconductor (MOS) capacitors, fabricated by evaporating patterned Al electrodes directly on top of the Hf-based oxide films and painting a GaIn eutectic alloy onto the back of the Ge substrates to form Ohmic contacts.[10]

III. RESULTS AND DISCUSSION

O K_1 edge XAS spectra, corresponding to samples of HfO_2 and HfSiON deposited on Ge (100) and annealed at 800 °C, are shown in Fig. 1. Normalization of the O K_1 edge spectra was performed by subtracting a straight-line background from the raw data and subsequently scaling the difference between the pre- and postedge levels to an arbitrary, but uniform, value. The relative intensities of the various peaks in these normalized O K_1 edge spectra reflect the molecular orbital bonding symmetries and C-F splittings in the corresponding samples.[11] Specifically, one can relate qualitatively the relative changes in energy levels shown in these spectra with different proportions of Hf–O bonding, even though exact quantities cannot be determined. The bottom of Fig. 1 also includes second derivative analysis of the O K_1 edge spectra. Such analysis is sensitive to minute changes in the XAS spectral features, which is very useful in interpreting the C-F splittings and J-T distortions.[1] The Gaussian fits shown in Fig. 1 were performed, as indicated by the vertical dashed lines, by assigning to each Gaussian peak, which corresponds to a peak energy occurring in the respective second derivative spectrum analysis. The results of these Gaussian fits show unambiguously the C-F splitting, as well as the presence of J-T *d*-state degeneracy and its removal. The Gaussian fits are composed of (i) band edge defect states, (ii) HF 5*d* e_g states having twofold degeneracy, (iii) Hf 5*d* t_{2g} states having threefold degeneracy, and (iv) two features corresponding to Hf 6*s* and Hf 6*p* states, respectively. The t_2 and a_1 states of the O K_1 edge in HfSiON films, however, mix with the hybrid states of Si 3*sp* and O 2*p* via the incorporation of Si–O bonding.[12] It is for this reason that the t_2 and a_1 states of HfSiON are higher than those of HfO_2. It is interesting to note that J-T distortion is observed clearly in HfO_2 films annealed at 800 °C; whereas, the *d*-state degeneracy occurring in HfSiON films is not removed upon annealing at 800 °C. This indicates that the stability of both the physical and electronic structures of HfSiON is superior to that of HfO_2. The four band-edge defect states detected by second derivative O K_1 edge spectrum analysis, which represent the equivalent d^4 state for a divacancy structure.[13] These states below conduction band edge, *D*(cb), were deconvoluted by using two different Gaussian functions, restricted by the spectral resolution and the energy deviation between defect states.

The molecular orbital energy diagrams of annealed HfO_2 and HfSiON above the valence band are described by Fig. 2, which takes into consideration the local symmetries of the bonding environments and the molecular orbital hybridization occurring between Hf and O atoms.[14,15] The XAS spectra, for example, demonstrate that the molecular orbital structure of HfO_2 exhibits the characteristic sevenfold O coordination ($t_{2g}+a_{1g}+t_{1u}$) under a cubic symmetry[16] and that HfSiON exhibits fourfold O coordination (t_2+a_1) under a tetrahedral symmetry. The two diagrams contained in Fig. 2 also include the C-F splittings, J-T distortions, molecular orbital index, bonding type, and energy levels relative to the respective valence band edges. The discrete defect states, indicated by $D(\mathrm{cb})_1$ and $D(\mathrm{cb})_2$, are located at energy levels lying below the conduction band edge, above Fermi level, and therefore within the band gap of both HfO_2 and HfSiON. Additionally, the molecular orbital structure of HfO_2 shows the Hf 5*d*-state degeneracy removal by a cooperative J-T distortion.

Figures 3(a) and 3(b) depict the thermal evolution of the O K_1 spectra for both HfO_2 and HfSiON over a narrow energy region below the doubly degenerate Hf 5*d* conduction band edge states. The Gaussian fits shown therein identify two distinct defect states, which are located at similar energies. More specifically, these defect energy levels, $D(\mathrm{cb})_1$ and $D(\mathrm{cb})_2$, are located at 530.2 ± 0.2 eV and 528.7 ± 0.2 eV, respectively. We have reported previously that the $D(\mathrm{cb})_1$ defect results from Hf^{3+} states associated with oxygen divacancies, which cluster at grain boundaries,

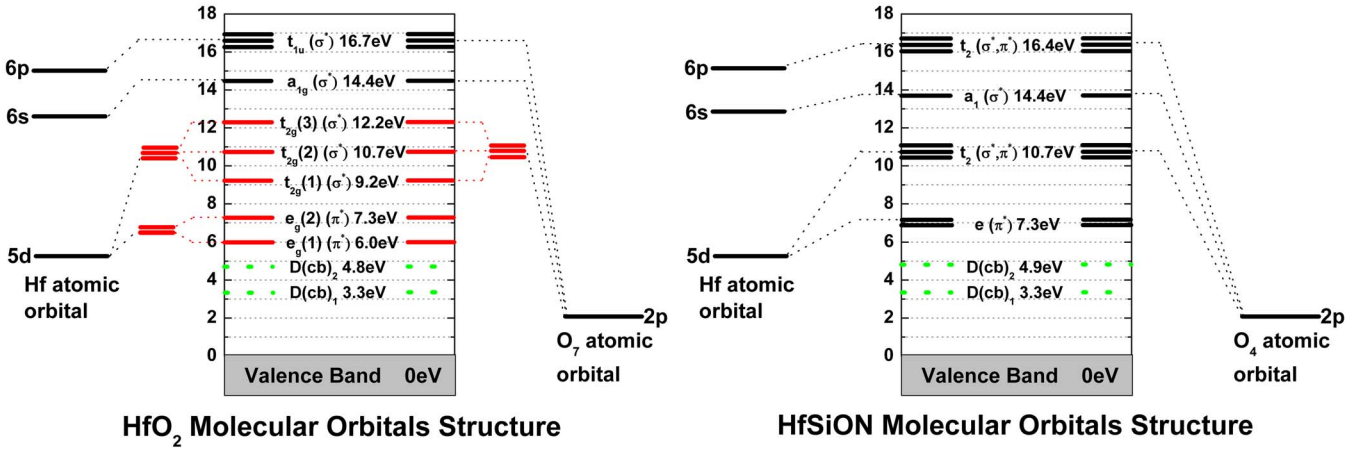

FIG. 2. (Color online) Molecular orbital energy diagram above valence band, considered by orbital hybridization between Hf atom and O atom and based on the experimental results of XAS O K_1 edge, for (a) HfO_2 and (b) HfSiON. The diagrams describe the C-F splittings, J-T distortion, the molecular orbital index, bonding type, and the energy level from valence band edge. We can know that the molecular orbital structure of HfO_2 has sevenfold O coordination ($t_{2g}+a_{1g}+t_{1u}$) under a cubic symmetry and that of HfSiON has fourfold O coordination (t_2+a_1) under a tetrahedral symmetry. $D(\mathrm{cb})_1$ and $D(\mathrm{cb})_2$ indicate the energy levels of two distinct defect states below the conduction band edge.

and that the $D(\mathrm{cb})_2$ defect results from Hf^{3+} and Ge^{3+} states associated with a divacancy, which occurs due to the incorporation of Ge into the film.[17,18] The density of defect states in HfO_2 is much larger than in HfSiON, regardless of the annealing temperature. This means that noncrystalline HfSiON films incorporate Si–O and Si–N bonding effectively in order to suppress these divacancy defects, as well as to hinder Ge incorporation into the films. Another reason for the relative reduction in defect states in HfSiON over HfO_2 involves the local atomic bonding symmetry of HfO_2. The sevenfold O coordination with respect to the Hf atoms in HfO_2 and the related J-T distortion enhance the possibility of Hf^{3+} divacancies and Ge diffusion via grain boundaries. The thermal evolution of the relative absorption in the defect states is shown in Fig. 3(c) as a function of PDA temperature and was calculated based on the relative area under each of the corresponding Gaussian curves, determined as in Figs. 3(a) and 3(b). The onset of clear changes in these trends appear over temperature ranges of approximately 575–625 °C and 625–675 °C in HfO_2 and HfSiON, respectively, which are related to the bond dissociation energies characterizing the interfacial GeO_xN_y layer between the high-κ oxide films and the Ge substrate. The difference in these transition temperatures is attributed to variations in structural stability, resulting from different atomic bonding symmetries and J-T distortions. The key result here, however, is that the density of defect states increases markedly at PDA temperatures between 650 and 700 °C in both HfO_2 and HfSiON, and it effectively becomes saturated at PDA temperatures in excess of 700 °C.

Capacitance-voltage (CV) characteristics in Fig. 4 show the correlation between the spectroscopic evolution of defect states and electrical characteristics as a function of PDA temperature. The normalized curves, shown as C/C_{OX} for 5 nm HfSiON on *n*-type Ge (100), are obtained by measuring their CV hysteresis at PDA temperatures ranging from 550 to 800 °C. Regardless of PDA temperature, both HfO_2 and HfSiON exhibit a clockwise hysteresis loop, indicating electron trapping in the oxide layer. The hysteresis loop for HfSiON, as depicted in Fig. 4(a), clearly achieves a minimum value at a PDA temperature of 650 °C. The effective trapped charge density, N_{EFF}, in the oxide layer can be calculated by using the following equation: $N_{\mathrm{EFF}}=C_{\mathrm{OX}}\Delta V_{\mathrm{FB,hysteresis}}/qA$, in which C_{OX} is the capacitance of the oxide layer, $\Delta V_{\mathrm{FB,hysteresis}}$ is the hysteresis in the flat band voltage, q is the electron charge, and A is the capacitor area.[19] The calculated effective trapped charge densities are plotted in Fig. 4(b) as a function of PDA temperature, and they demonstrate minimum values at temperatures of 600 and 650 °C in HfO_2 and HfSiON, respectively. This trend in electron trapping may be attributed in part to several causes. First, the band offset between these Hf-based high-κ dielectric oxides and the GeO_xN_y interfacial layer leads to electron trapping in the conduction band, caused by a quantum well-like region at their interface. This explanation is in agreement with the fact that at PDA temperatures below approximately 600–650 °C, the GeO_xN_y region persists.[20] Recent modeling, based on surface charge neutrality and carried out by Tsipas and Dimoulas,[21] also provides evidence for the existence of negatively charged states at the Ge surface and interface. The final contributions to electron trapping in this material system are attributed to Hf^{3+} states arising from oxygen divacancies clustered at grain boundaries and to Hf^{3+} and Ge^{3+} states caused by the incorporation of Ge into the films. Furthermore, the observed shift in flat band voltage (V_{FB}) is in the positive direction as PDA temperature increases, which indicates that the density of negatively charged traps increases with temperature. This phenomenon is correlated with changes in the number of O divacancies present at grain boundaries in the film,[22] which, as demonstrated by the XAS spectra, exhibit an increase as a function of PDA temperature until approximately 700 °C.

IV. CONCLUSION

In summary, changes in the molecular orbital structures of HfO_2 and HfSiON high-κ dielectric oxides deposited on *n*-type Ge (100) substrates were investigated by examining

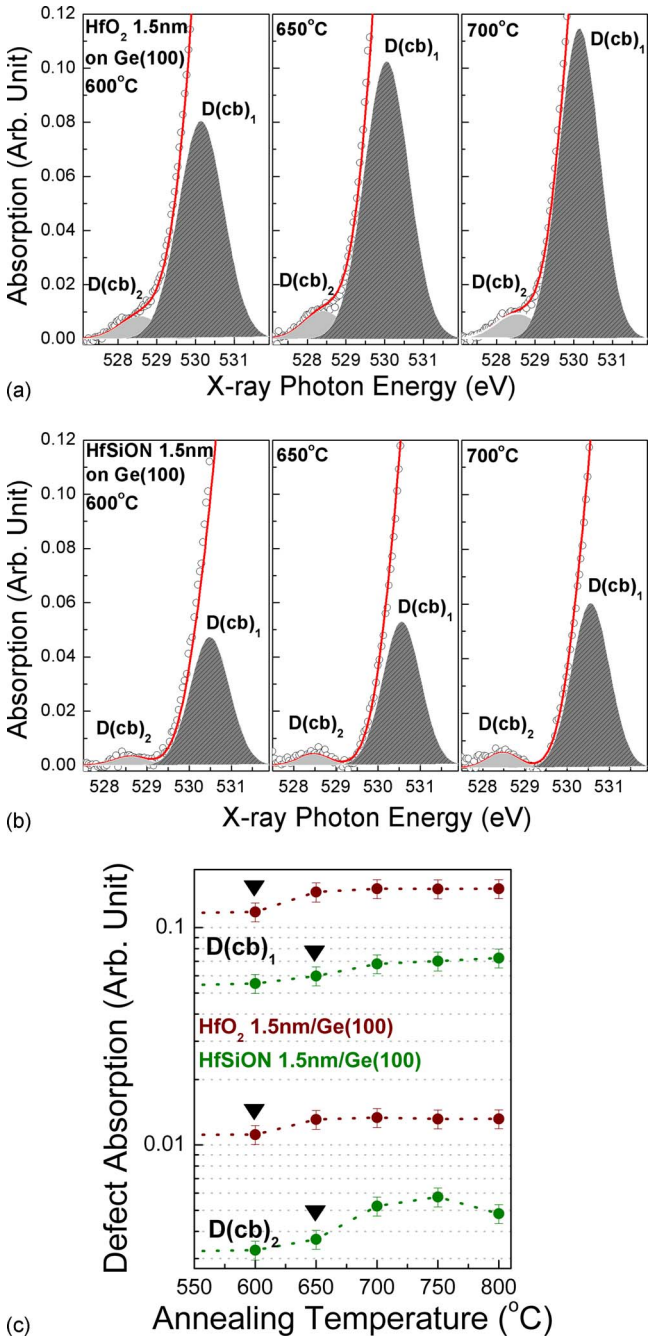

FIG. 3. (Color online) Thermal evolution of the O K_1 spectra for (a) HfO_2 and (b) HfSiON over a narrow energy region below the doubly degenerate HF 5*d* conduction band edge states as a function of PDA temperature. Two deconvoluted peaks, labeled $D(\mathrm{cb})_1$ and $D(\mathrm{cb})_2$, indicate the defect states determined by Gaussian fits of the XAS O K_1 edge spectra. (c) Thermal evolution of relative absorption for two distinct defect states, calculated by Gaussian fits in (a) and (b). The arrows indicate the onsets of clear change in theses trends of each defect state.

O K_1 edge spectra obtained via XAS. The C-F splittings and J-T *d*-state degeneracy removal resulting from cooperative distortions are identified through second derivative analysis of these O K_1 edge spectra, and they are interpreted within the context of the symmetry of local bonding environments. The origins of the two discrete defect states below the conduction band edge are identified and analyzed qualitatively. In addition, the thermal evolution of defect states are shown to be correlated with the presence of Ge^{3+} states, resulting

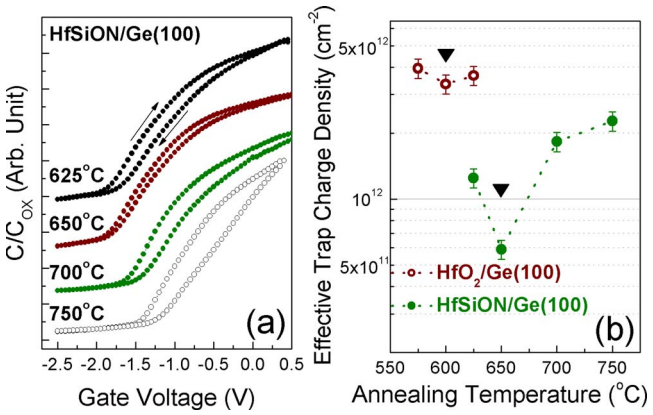

FIG. 4. (Color online) (a) CV characteristics of *n*-type MOS capacitor of 5 nm HfSiON on *n*-type Ge (100), normalized by C/C_{OX}, as a function of PDA temperature. The arrow provides the direction of hysteresis, indicating the clockwise hysteresis loop. (b) Thermal evolution of effective trap charge density, calculated by the hysteresis offset of CV characteristics.

from Ge migration, and with Hf^{3+} states, associated with O divacancies residing near grain boundaries in these films. The higher thermal stability of HfSiON dielectric films, which exhibit fourfold O coordination, corresponds to fewer defect states with respect to HfO_2 films, which exhibit sevenfold O coordination and a J-T distortion. These defect states below the conduction band edge, in addition to the quantum well-like structure in the conduction band at the high-κ/GeO_xN_y interface, induce an electrically active effective electron charge trapping.

[1]G. Lucovsky, H. Seo, S. Lee, L. B. Fleming, M. D. Ulrich, J. Lüning, P. Lysaght, and G. Bersuker, Jpn. J. Appl. Phys., Part 1 **46**, 1899 (2007).
[2]M. Ieong, B. Doris, J. Kedzierski, K. Rim, and M. Yang, Science **306**, 2057 (2004).
[3]C. O. Chui, F. Ito, and K. Saraswat, IEEE Trans. Electron Devices **53**, 1501 (2006).
[4]H. Shang, H. Okorn-Schmidt, K. K. Chan, M. Copel, J. A. Ott, P. M. Kozlowsi, S. E. Steen, H.-S. P. Wong, E. C. Jones, and W. E. Haensch, Tech. Dig. - Int. Electron Devices Meet. **2002**, 441.
[5]K. Prabhakaran and T. Ogino, Surf. Sci. **325**, 263 (1995).
[6]K. B. Chung, C. N. Whang, M.-H. Cho, and D.-H. Ko, Appl. Phys. Lett. **88**, 111913 (2006).
[7]S. Guha and V. Narayanan, Phys. Rev. Lett. **98**, 196101 (2007).
[8]V. A. Gritsenko, J. B. Xu, R. W. Kwok, Y. H. Ng, and I. H. Wilson, Phys. Rev. Lett. **81**, 1054 (1998).
[9]D. E. Aspnes and A. A. Studna, Appl. Phys. Lett. **39**, 316 (1981).
[10]S. F. Galata, E. K. Evangelou, Y. Panayiotatos, A. Sotiropoulos, and A. Dimoulas, Microelectron. Reliab. **47**, 532 (2007).
[11]J. Stöhr, *NEXAFS Spectroscopy* (Springer, New York, 1991).
[12]Z. Y. Wu, F. Jollet, and F. Seifert, J. Phys.: Condens. Matter **10**, 8083 (1998).
[13]G. Lucovsky, K. B. Chung, J.-W. Kim, and D. Nordlund, unpublished.
[14]H. B. Gray, *Electrons and Chemical Bonding*, (Addison-Wesley, Reading, MA, 1964).
[15]F. A. Cotton, *Chemical Applications of Group Theory*, 3rd ed., (Wiley-Interscience, New York, 1990).
[16]R. Ruh and P. W. R. Corfield, J. Am. Ceram. Soc. **53**, 126 (1970).
[17]K. B. Chung, H. Seo, J. P. Long, and G. Lucovsky, Appl. Phys. Lett. **93**, 182903 (2008).
[18]G. Lucovsky, J. P. Long, K.-B. Chung, H. Seo, B. Watts, R. Vasic, and M. D. Ulrich, J. Vac. Sci. Technol. B **27**, 294 (2009).
[19]P.-C. Jiang and J. S. Chen, J. Electrochem. Soc. **151**, G751 (2004).
[20]G. Lucovsky, S. Lee, J. P. Long, H. Seo, and J. Lüning, Microelectron. Eng. **86**, 224 (2009).
[21]P. Tsipas and A. Dimoulas, Appl. Phys. Lett. **94**, 012114 (2009).
[22]J. L. Gavartin, D. Munoz, A. L. Shluger, G. Bersuker, and B. H. Lee, Appl. Phys. Lett. **89**, 082908 (2006).